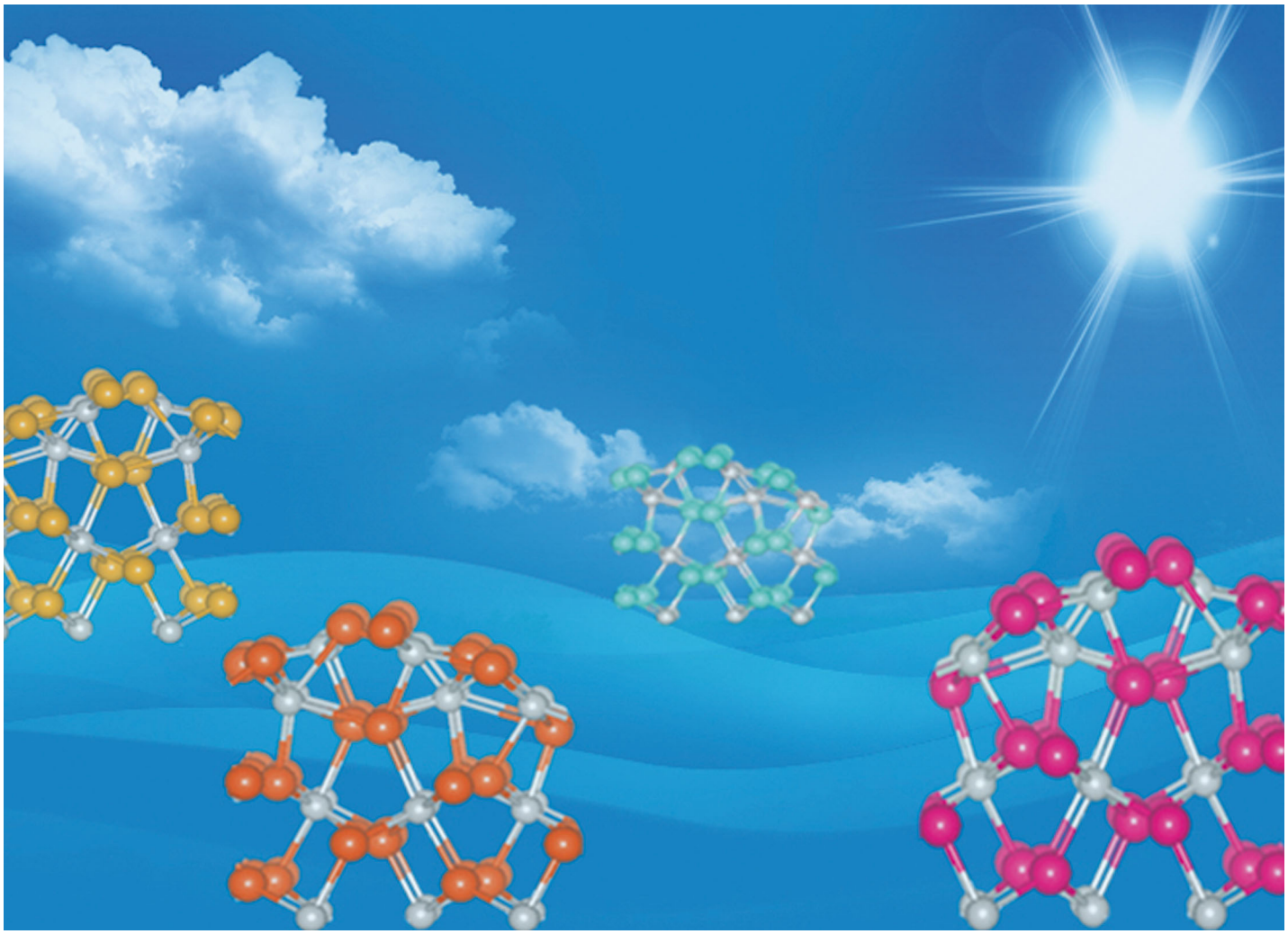

Showcasing work from the Computational Materials Discovery Lab, Moscow Institute of Physics and Technology, Russia.

Title: The unexpectedly rich reconstructions of rutile TiO_2(011)-(2 × 1) surface and the driving forces behind their formation: an *ab initio* evolutionary study

The rich chemistry of TiO_2(011)-(2 × 1) is uncovered. Titanyl-TiO_2 and titanyl-Ti_2O_3 reconstructions rationalize experimental findings. The predicted MF(111)-TiO reconstruction is more reasonable than the previously proposed MF(111)-TiO_3 model. The richness of surface phases is driven by thermodynamic conditions and surface stress release. More importantly, this paper reveals the roles of metastability on surface structures, significantly broadening our current understanding.

As featured in:

See Qinggao Wang *et al.*, *Phys. Chem. Chem. Phys.*, 2016, **18**, 19549.

ROYAL SOCIETY OF CHEMISTRY

Registered charity number: 207890

PCCP

PAPER

Cite this: *Phys. Chem. Chem. Phys.*, 2016, **18**, 19549

The unexpectedly rich reconstructions of rutile TiO_2(011)-(2 × 1) surface and the driving forces behind their formation: an *ab initio* evolutionary study†

Qinggao Wang,*[ab] Artem R. Oganov,[cade] Oleg D. Feya,[a] Qiang Zhu[d] and Dongwei Ma[b]

Received 22nd February 2016,
Accepted 6th April 2016

DOI: 10.1039/c6cp01203e

www.rsc.org/pccp

In this paper, we employ state-of-the-art theoretical approaches to elucidate the structures of the (011) surface of rutile (R-)TiO_2. An unexpectedly rich chemistry has been uncovered. Titanyl-TiO_2 and titanyl-Ti_2O_3 reconstructions can be used for rationalizing the experimental findings, matching the STM images and the changes in the band gap. From the viewpoint of thermodynamics, the predicted MF(111)-TiO reconstruction is more reasonable than the previously proposed MF(111)-TiO_3 model, although there is a structural similarity. The richness of surface phases, the formation of which is driven by thermodynamic conditions and surface stress release, implies the multifunctionality of the R-TiO_2(011) surface. After the clarification of TiO_2(011) and TiO_2(110) surface structures {*PRL*, 2014, **113**, 266101} (the most important surfaces of rutile), the origin of the Brønsted acidity of R-TiO_2, which has remained a mystery at the atomic level, can also be addressed in the near future.

1 Introduction

TiO_2 polymorphs (rutile, anatase and brookite) are promising materials for photocatalytic water splitting and degradation reactions of organic pollutants,[1,2] and their surface structures have been investigated extensively due to their correlations with reaction mechanisms.[3–5] The (011) face of rutile (R-)TiO_2, the second most abundant face of its crystals, has been explored in relation to oxidation[3,4] or reduction[5] sites. However, structural uncertainties hamper the understanding of the multifunctionality of the R-TiO_2(011) surface. Surface reconstructions must be resolved for any further progress.

Previously, Noguera *et al.* pointed out that the surface structures of metal oxides are sensitive to the environment and are challenging to study by either experiments or simulations separately.[6–8] For the TiO_2 rutile(011) surface, R-TiO_2(011)-(2n × 1) (n = 1–5) reconstructions have been obtained after annealing sputtered samples,[9–12] but the R-TiO_2(011)-(2 × 1) reconstruction was most frequently observed. After irradiation with 300 eV electrons, the site-specific desorption of oxygen atoms of the R-TiO_2(011)-(2 × 1) resulted in a self-organized structure containing one-dimensional streaks of oxygen vacancies,[13] which may enhance photocatalytic activity. Tao *et al.* discovered that the band gap of a metastable R-TiO_2(011)-(2 × 1) structure (2.1 eV) matches the energy of visible light,[14] potentially enabling photocatalysis with visible light. According to these experimental results, the structures of the R-TiO_2(011)-(2 × 1) reconstruction are diverse, and they are closely correlated with photocatalytic activity. However, due to the limitations of common experimental and theoretical methods, no one has ever attempted to clarify them systematically.

Until now, "titanyl-TiO_2",[15–17] "MF(111)-TiO_3"[11] and "B(001)-TiO_2"[10,18] models were proposed for the R-TiO_2(011)-(2 × 1) reconstruction by the combination of experiments and simulations, respectively. The titanyl-TiO_2 model has titanyl groups on both sides of the surface oxygen rows,[15] but it was questioned due to its high surface energy.[11] Non-contact atomic force microscopy studies indicated that the R-TiO_2(011)-(2 × 1) reconstruction exhibits rowlike features along the [01−1] direction.[11] The MF(111)-TiO_3 model, terminated by (111) and (−111) microfacets, was proposed.[11] Yet, this oxygen-rich model is impossible from the viewpoint of thermodynamics, since the R-TiO_2(011)-(2 × 1) reconstruction was observed in an oxygen-deficient environment,

[a] *Moscow Institute of Physics and Technology, 9 Institutskiy Lane, Dolgoprudny City, Moscow Region, 141700, Russia. E-mail: wangqinggao1984@126.com*
[b] *Department of Physics and Electrical Engineering, Anyang Normal University, Anyang, Henan Province, 455000, People's Republic of China*
[c] *Skolkovo Institute of Science and Technology, Skolkovo Innovation Center, 3 Nobel St., Moscow 143026, Russia*
[d] *Department of Geosciences and Center for Materials by Design, Stony Brook University, Stony Brook, New York 11794, USA*
[e] *School of Materials Science and Engineering, Northwestern Polytechnical University, Xi'an, Shanxi 710072, People's Republic of China*

† Electronic supplementary information (ESI) available. See DOI: 10.1039/c6cp01203e

i.e., in a vacuum at high temperature. Afterwards, the B(001)-TiO_2 model, displaying the features of brookite TiO_2(001), was proposed,[10,18] and it has a lower surface energy according to density functional theory (DFT) calculations.[10,18] Moreover, this model is in agreement with several experimental findings.[19,20] Although the above results are insightful, their incompleteness, mismatching rich structures of the R-TiO_2(011)-(2 × 1) reconstruction obtained in experiments, is obvious when considering the subsequent experimental findings. For example, a metastable R-TiO_2(011)-(2 × 1) structure was found after the proposal of these atomic models.[14,21]

To better understand the rich structures of the R-TiO_2(011)-(2 × 1) reconstruction, we need to investigate the driving forces behind their formation. Certainly, surface energy is the criterion for thermodynamic stability of a surface. However, metastability can play a role and the formation of TiO_2 rutile(011) reconstructions is determined by both thermodynamic and kinetic factors, since the actual surface phase is the result of interplay between Ti deposition, O_2 gas pressure, oxygen vacancies and Ti interstitials (*i.e.*, certain environment and the history of samples). The formation of surface structures must be kinetically viable under the preparation conditions.[22] In fact, a metastable surface structure has been obtained experimentally, as reported by Tao *et al.*[14] Usually, stability of surface phases is described as being due to reduction of the surface energy, surface stress, or of the number of dangling bonds. For metal surfaces, reconstructions are better described as stress-driven, *e.g.*, Au(111)-(23 × $\sqrt{3}$),[23] while the reduction of the density of dangling bonds drives the reconstruction of semiconductor surfaces, *e.g.*, Si(100)-(2 × 1).[24] Different from the Au(111) and Si(100) surfaces, the driving forces behind TiO_2 surface reconstructions are more complicated. As already reported, the reconstructions of the R-TiO_2(110) surface,[25] microfaceting missing-row reconstruction of R-TiO_2(011)-(2 × 1)[11] and added-molecule reconstruction of anatase TiO_2(001)-(1 × 4)[26] are driven by the change in thermodynamic conditions, reduction of the density of dangling bonds and release of surface stress, respectively. The richness of the structures of the R-TiO_2(011)-(2 × 1) reconstruction suggests that there can be manifold driving forces behind this reconstruction. Is this true?

In short, the current understanding of the R-TiO_2(011)-(2 × 1) reconstruction is still controversial and incomplete. In this paper, we use an advanced variable-composition surface structure prediction method implemented in the USPEX package, coupled with *ab initio* simulations, to investigate the structures of the R-TiO_2(011) surface, and the driving forces behind the formation of these structures. In this way, a complete and renewed understanding was obtained.

2 Computational methodology

To explore all stable reconstructions of the R-TiO_2(011) surface, we used the USPEX code,[27–30] which has been successfully applied to bulk crystals,[28] nanoparticles,[30] surfaces[25,29] and polymers.[31] In our recent paper, we gave a brief introduction of the surface module.[25] In this paper, we allowed for index-4 multiplications of the surface unit cell (*i.e.* 1 × 1, 1 × 2, 2 × 1, 1 × 3, 3 × 1, 2 × 2, 1 × 4 and 4 × 1), with up to two Ti and four O atoms per single surface unit cell. To avoid dipoles being artificially introduced into computational models, the atomic stacking sequence of the substrate was chosen according to the test calculations of an unreconstructed TiO_2 rutile(011) surface. Each supercell consisted of a slab of four TiO_2 layers (a thickness of about 9.20–10.10 Å, the uppermost 3.5 Å of which were allowed to relax) and a vacuum layer of 13 Å. For the lowest-energy structures we also performed more accurate calculations, in which only their bottom TiO_2 layers were fixed during relaxation. This type of surface models (*i.e.*, asymmetric models) has been extensively adopted in the past.[15,18]

The VASP code[32–34] was invoked for local optimizations during the USPEX calculation. However, certain important metastable structures may be left out, since USPEX is a global optimization method. In this paper, the pure VASP calculations were also performed for the previously proposed metastable structures if they did not appear in the USPEX calculations. Since the generalized gradient approximation (GGA) is known to be affected by the self-interaction error,[35] the electron exchange and correlation were treated using the GGA+U ($U - J$ = 4.1 eV) method, similar to recently published papers.[36,37] And these calculations were spin-polarized. The projector-augmented wave method was applied to treat core electrons,[38] while valence orbitals were expanded in plane waves with a 480 eV kinetic energy cutoff. Γ-centered 2π × 0.09 $Å^{-1}$ grids were chosen for Brillouin zone integrations. Dipole corrections were adopted to cancel interactions between slabs and their periodic images.[39,40] Structural relaxations progressed until forces on all atoms were less than 0.001 eV $Å^{-1}$.

Surface energy characterizes thermodynamic stability of each reconstruction. Here, we define surface energies of the unrelaxed stoichiometric R-TiO_2(011) and a relaxed stoichiometric or nonstoichiometric R-TiO_2(011) structure

$$\gamma_u = (E_{st}^u - E_b)/(2A_L), \quad (1a)$$

$$\gamma = (E_{sur} - E_b - \Delta n_i \mu_i)/A_L - \gamma_u, \quad (1b)$$

respectively. As a function of strain, E_{st}^u, E_b and E_{sur} are the total energies of the supercells of the unrelaxed stoichiometric R-TiO_2(011), R-TiO_2 bulk, and a relaxed stoichiometric or non-stoichiometric R-TiO_2(011) structure, respectively. Δn_i is the stoichiometry deviation of a R-TiO_2(011) structure, and μ_i is the chemical potential of O or Ti species. A_L is the area of a R-TiO_2(011) surface cell in the unstrained state. It should be noticed that the uppermost atomic layer and the lowermost one must be equal when one uses the formula (1a).

Chemical potentials μ_O and μ_{Ti} satisfy the following boundary conditions: $\mu_O \leq 1/2\mu_{O_2}$, $\mu_{Ti} \leq \mu_{Ti}^{bulk}$ and $\mu_{Ti} + 2\mu_O = E_{TiO_2}$, where E_{TiO_2} is the total energy of R-TiO_2 bulk per unit cell. Accordingly, eqn (1b) can be rewritten as

$$\gamma = [E_{sur} - E_b - \mu_O(n_O - 2n_{Ti})]/A_L - \gamma_u, \quad (2)$$

where n_O and n_{Ti} are the numbers of O and Ti atoms of a R-TiO_2(011) structure, respectively. Accordingly, a surface phase diagram can be constructed.

To recast this surface phase diagram, the μ_{Ti}-independent and stoichiometry deviation terms are defined as

$$\gamma_0 = [E_{sur} - E_b]/A_L,\ \Delta s = (n_O - 2n_{Ti})/A_L, \quad (3)$$

respectively. In the coordinate system of γ_0 and Δs, each R-TiO_2(011) structure is represented as a point. Thermodynamically stable structures form a convex hull. Points above it are metastable.

Stoichiometric deviations should correlate with thermodynamic conditions. Given that stable R-TiO_2(011) structures are in equilibrium with the O_2 gas, μ_O can be defined as[25,41]

$$\mu_O = 1/2E_{O_2} + \Delta\mu_O(T,P) = 1/2[E_{O_2} + \Delta H_{O_2}(T,P^0) - T\Delta S_{O_2}(T,P^0) + k_B T\ln(P/P^0)], \quad (4)$$

where k_B and P^0 are the Boltzmann constant and standard atmospheric pressure, respectively. E_{O_2} is the total energy of an isolated O_2 molecule, and is evaluated through spin-polarized calculations. ΔH_{O_2} and $T\Delta S_{O_2}$ are the contributions of enthalpy and entropy at ambient pressure, respectively, and they could be taken from a thermodynamic database.[42] $k_B T\ln(P/P^0)$ is the contribution of the partial pressure of O_2 gas. This allows us to use O chemical potential instead of the temperature and O_2 partial pressure as basic thermodynamic variables.

As was mentioned before, the release of surface stress is a possible driving force behind the formation of R-TiO_2(011)-(2 × 1) structures. Surface stress is the first derivative of surface energy with respect to strain,[43,44] *i.e.*,

$$\sigma_{ij} = A_L^{-1}[\partial(\gamma A)/\partial\varepsilon_{ij}] = \gamma\delta_{ij} + \partial\gamma/\partial\varepsilon_{ij}. \quad (5)$$

ε_{ij} is the applied strain on a R-TiO_2(011) structure.

3 Results and discussion

3.1 Driving forces behind the formation of B(001)-TiO_2 and titanyl-TiO_2 reconstructions

According to our test calculations for the unreconstructed TiO_2 rutile(011) surface (as seen in the ESI†), slab models of the unreconstructed R-TiO_2(011) structure, including that of 4 TiO_2 atomic layers, are thick enough. The changes in surface energy are within 0.02 eV when the thickness of slab models increases from three TiO_2 atomic layers to seven.

Surface energy reflects thermodynamic stability of a surface structure, and thus this physical quantity is quite important for the understanding of surface reconstruction. The unreconstructed R-TiO_2(011) surface is more stable than the B(001)-TiO_2 and titanyl-TiO_2 reconstructions (Table 1). In agreement with published papers,[10,18,37] the GGA calculations indicate that the surface energy of B(001)-TiO_2 reconstruction is a little lower than that of the unreconstructed R-TiO_2(011) surface (0.06 eV per surface unit cell). This result indicates that our atomic models are thick enough, and thus they can describe the relative stability of reconstructed and unreconstructed TiO_2 rutile(011) structures. Furthermore, the uncertainty in energetics, caused by the computational methods (*i.e.*, the GGA+*U* or GGA), does not alter our conclusions. The titanyl-TiO_2 reconstruction is certainly a metastable structure, and this conclusion is independent of the computational methods (*i.e.*, the GGA+*U* or GGA). Without doubt, reconstructed R-TiO_2(011) structures could not be well understood through analyses of surface energies only, since the kinetics also play a role in their formation.

Table 1 Surface energy (γ) and surface stress (σ_{ii}) [in eV/(1 × 1) unit cell] of the titanyl-TiO_2, B(001)-TiO_2 reconstruction, and unreconstructed R-TiO_2(011) surface. The subscripts "*xx*" and "*yy*" denote the components of surface stress tensor. Here, *x* and *y* axes correspond to the [100] and [01−1] directions of rutile TiO_2

Structures	γ	σ_{xx}	σ_{yy}
B(001)-TiO_2	2.09	7.06	12.90
Titanyl-TiO_2	2.41	6.18	9.93
R-TiO_2(011)	1.95	10.36	10.93

Atoms at the surface feel a rather extreme environment, since their coordination number becomes smaller compared to bulk, and the mismatch between surface and bulk causes surface stress. To explore the driving forces behind surface reconstructions, we calculate the surface stress of the B(001)-TiO_2 reconstruction, titanyl-TiO_2 reconstruction and R-TiO_2(011) surface along the [100] and [01−1] directions (Table 1). Surface stresses of the unreconstructed R-TiO_2(011) surface are 10.36 and 10.93 eV per surface unit cell along the [100] and [01−1] directions, respectively. Compared with the unreconstructed R-TiO_2(011) surface (10.36 eV per surface unit cell along the [100] direction), the surface stress of the B(001)-TiO_2 reconstruction along the [100] orientation (7.06 eV per surface unit cell) significantly decreases, but this is compensated by increased tensile stress along the [01−1] direction. As expected, when compared with the unreconstructed TiO_2 rutile(011) surface, the surface stress of B(001)-TiO_2 reconstruction along the [01−1] direction increases by 1.97 eV for per surface unit cell. In a previous study, a similar phenomenon was observed for the added-molecule reconstruction of anatase TiO_2(001)-(1 × 4),[26] and the driving force behind this reconstruction was concluded to be stress-driven. Accordingly, the formation of the B(001)-TiO_2 reconstruction is also stress-driven.

The formation of titanyl-TiO_2 reconstruction is also stress-driven. Its surface stress along the [100] direction is 6.18 eV per surface unit cell, much smaller than that of the unreconstructed TiO_2 rutile(011) surface. Different from the B(001)-TiO_2 reconstruction, trenches of the titanyl-TiO_2 reconstruction are beneficial to release surface stress. Attributed to these trenches, the decrease of tensile stress along the [100] direction (compared with the unreconstructed TiO_2 rutile(011) surface) does not lead to additional tensile stress along the [01−1] direction. Therein, the σ_{yy} value of titanyl-TiO_2 reconstruction (9.93 eV per surface unit cell) is smaller than that of the unreconstructed TiO_2 rutile(011) surface. In fact, the missing-row pattern is a common mechanism for surface reconstruction, such as the (3 × 1) and (4 × 1) reconstructions of the O/Nb(100) system.[45]

To sum up, the formation of B(001)-TiO_2 and titanyl-TiO_2 reconstructions is stress-driven, and the kinetic factor should play an important role since these structures are metastable.

3.2 *Ab initio* evolutionary exploration of R-TiO_2(011) reconstructions

The predicted low-energy structures and their thermodynamics are summarized in Fig. 1, *i.e.*, surface energies as a function of stoichiometric deviation (Δs) and O chemical potential ($\Delta\mu_O$). Stoichiometric deviations of stable structures change with O chemical potential, from the unreconstructed R-TiO_2(011) surface (-3.46 eV $\leq \Delta\mu_O \leq 0$ eV) to a "MF(111)-TiO" reconstruction (-4.47 eV $\leq \Delta\mu_O \leq -3.46$ eV), and to a "MR-TiO" reconstruction (-4.96 eV $\leq \Delta\mu_O \leq -4.47$ eV). Note that close surface energies imply competition between the B(001)-TiO_2 reconstruction and unreconstructed R-TiO_2(011) surface, as well as between the MF(110)-TiO and MR-TiO reconstructions.

The previously proposed models (*i.e.*, the titanyl-TiO_2,[15–17] MF(111)-TiO_3[11] and B(001)-TiO_2[10,18] reconstructions) are quite insightful, and they share similarities with the presently predicted R-TiO_2(011)-(2 × 1) reconstructions, as analyzed in the following.

Titanyl-Ti_2O_3. The earlier proposed titanyl-TiO_2[15] model, having titanyl groups on both sides of surface oxygen rows, is shown in Fig. 2a. Titanyl bonds (1.66 Å) are 0.30 Å shorter than typical Ti–O bonds, in agreement with the reported value.[15] The surface Ti layer has almost zero corrugation (0.01 Å). Different from the titanyl-TiO_2 model, the predicted titanyl-Ti_2O_3 structure contains titanyl groups on one side of surface oxygen rows, as shown in Fig. 2b. The bond length of titanyl groups (1.67 Å) is approximately the same as that in the titanyl-TiO_2 model, but the corrugation of the surface Ti layer (0.83 Å) is significant.

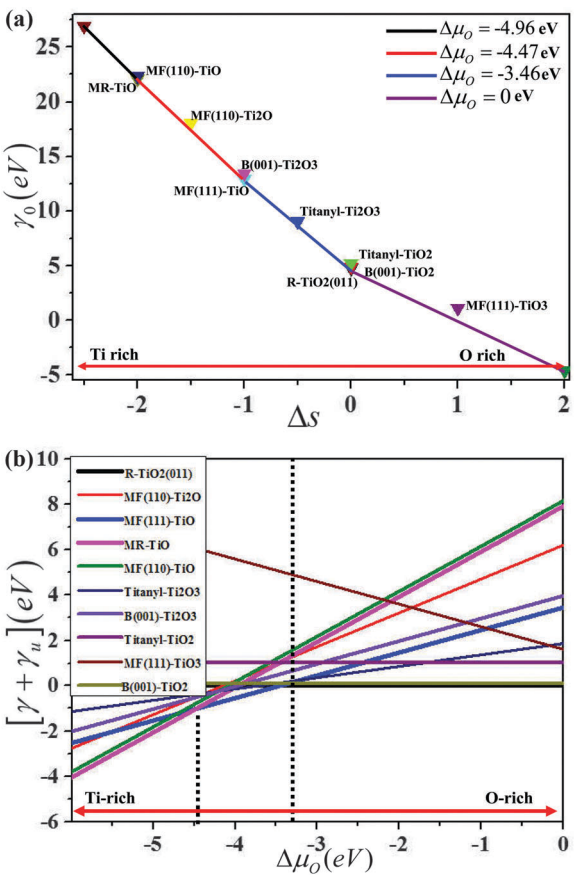

Fig. 1 Surface phase diagrams of the R-TiO_2(011) surface as a function of (a) stoichiometric deviation Δs and (b) relative O chemical potential $\Delta\mu_O$. As a constant, γ_u is introduced for convenience.

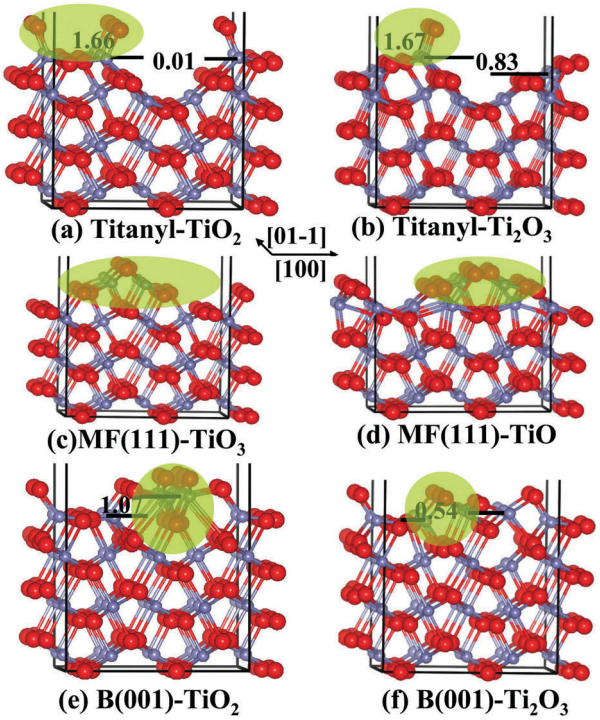

Fig. 2 Side view of (a) previously proposed titanyl-TiO_2,[15] (b) predicted "titanyl-Ti_2O_3", (c) previously proposed MF(111)-TiO_3,[11] (d) predicted "MF(111)-TiO", (e) previously proposed B(001)-TiO_2,[18] and (f) predicted "B(001)-Ti_2O_3" reconstructed structures. Small gray and big red spheres represent Ti and O atoms, respectively. Essential structural features are highlighted.

Experimentally, a self-organized structure containing one-dimensional streaks of oxygen vacancies was formed after the irradiation of a R-TiO_2(011)-(2 × 1) structure with 300 eV electrons.[13] Compared with the titanyl-TiO_2 model, the predicted titanyl-Ti_2O_3 reconstruction loses one side of titanyl groups, *i.e.*, it can be viewed as containing one-dimensional streaks of oxygen vacancies. Therefore, the titanyl-TiO_2 and titanyl-Ti_2O_3 reconstructions probably correspond to R-TiO_2(011)-(2 × 1) structures formed before and after irradiating with electrons,[13] respectively.

MF(111)-TiO. The previously proposed MF(111)-TiO_3[11] model and the predicted MF(111)-TiO structure share similarities, and both of them are terminated by (111) and (−111) microfacets. However, their geometry and chemistry are different. For example, the interlayer distance between the surface and subsurface Ti atoms is 1.24 Å for the MF(111)-TiO reconstruction, while that for the MF(111)-TiO_3 model is 2.38 Å.

Experimentally, the microfaceting (MF) reconstruction was obtained through heating of a sample at 800 °C in a vacuum,[11]

i.e., in an environment of low μ_O. The corresponding structure should be O-deficient from the viewpoint of thermodynamics. This explains why the predicted MF(111)-TiO reconstruction is more stable than the previously proposed MF(111)-TiO_3[11] model.

B(001)-Ti_2O_3. For the B(001)-TiO_2 reconstruction, the calculated surface Ti–O bond lengths (1.84 and 1.93 Å) are less asymmetric than the reported values of Torrelles *et al.*[18] (1.76 and 1.62 Å) and Gong *et al.*[10] (1.96 and 2.28 Å), but agree well with a LEED investigation.[19] Compared with the B(001)-TiO_2 reconstruction, the predicted B(001)-Ti_2O_3 reconstruction (Fig. 2f) loses surface and subsurface oxygen rows along the [01−1] direction. The corrugation of the surface Ti atomic layer is 1.07 Å for the previously proposed B(001)-TiO_2 model, while that of the presently predicted B(001)-Ti_2O_3 structure is 0.54 Å. These results indicate that surface distortion of the B(001)-TiO_2 reconstruction is significantly reduced through introduction of oxygen vacancies, corresponding to further release of surface stress.

Other R-TiO_2(011)-(2 × 1) reconstructions. Low-energy "MR-TiO", "MF(110)-TiO" and "MF(110)-Ti_2O" structures are also predicted, as shown in Fig. 3. Compared with the unreconstructed R-TiO_2(011) surface, the MR-TiO reconstruction (Fig. 3b) loses O rows at the surface, and subsurface O rows migrate to the surface. The interlayer distance between the surface and subsurface Ti atomic layers is 1.88 Å, and the corrugation of the surface Ti atomic layer is 0.69 Å. These results suggest that the stoichiometric deviation of this R-TiO_2(011)-(2 × 1) reconstruction is accompanied by a significant surface distortion.

The MF(110)-TiO and MF(110)-Ti_2O reconstructions are microfaceted structures with trenches, and their stoichiometries at the surface are TiO and Ti_2O, respectively. Similar to the titanyl-TiO_2 reconstruction, these trenches should be beneficial to release surface stress.

In brief, the formation of the nonstoichiometric structures of the R-TiO_2(011)-(2 × 1) reconstruction should be driven by the combination of surface energies, their dependence on chemical potential, and by surface stress release.

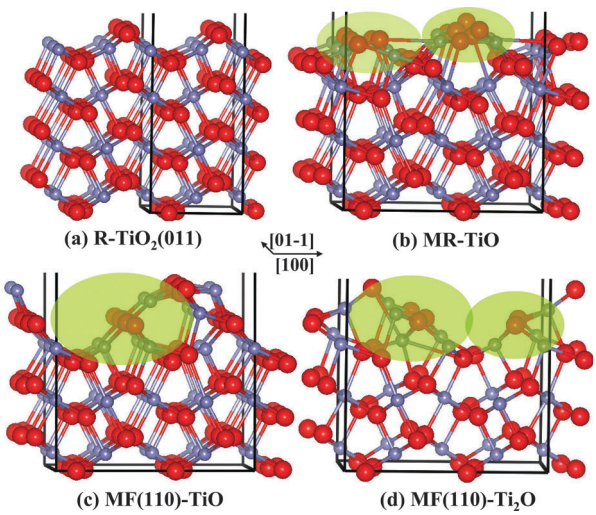

Fig. 3 Side view of (a) the unreconstructed R-TiO_2(011) surface, (b) "MR-TiO", (c) "MF(110)-TiO" and (d) "MF(110)-Ti_2O" reconstructed structures. Structural features are highlighted.

3.3 Simulated STM images of R-TiO_2(011)-(2 × 1) reconstructions

How do the predicted R-TiO_2(011)-(2 × 1) structures agree with the knowledge that has been obtained in experiments? To solve this question, scanning tunneling microscopy (STM) images were simulated using the Tersoff method.[46] Therein, an energy window of empty states and the distance above the surface are about 1.2 eV and 2 Å, respectively. Lighter shades correspond to regions with denser unoccupied states.

As shown in Fig. 4a, the zigzag chains of round spots in the simulated STM image of the MF(111)-TiO correspond to the unoccupied states of surface Ti atoms, while those of the titanyl-TiO_2 (Fig. 4b, as illustrated by blue lines) correspond to surface O atoms. Both the MF(111)-TiO and titanyl-TiO_2 reconstructions are in agreement with experimental observations,[9–11,13,15–17] *i.e.*, zigzag patterns in the STM images.

The bright spots in Fig. 4b also show a distorted hexagonal pattern (as illustrated by the red lines), which is the same as the experimental STM image (Fig. 4d) reported by Tao *et al.*,[14] corresponding to a R-TiO_2(011)-(2 × 1) structure with a band gap of 2.1 eV. This agreement suggests that the titanyl-TiO_2 is the structure obtained by Tao *et al.*[14]

As mentioned, bright spots in the simulated STM image of titanyl-TiO_2 (Fig. 4b) are arranged in zigzag rows, while those of the titanyl-Ti_2O_3 (Fig. 4c) are arranged in straight rows. These results are in agreement with the reported STM images of R-TiO_2(011)-(2 × 1) before and after irradiating with electrons (Fig. 4e and f).[13] Consequently, we confirm that the titanyl-TiO_2 and titanyl-Ti_2O_3 are the R-TiO_2(011)-(2 × 1) structures before and after irradiating with electrons,[13] respectively.

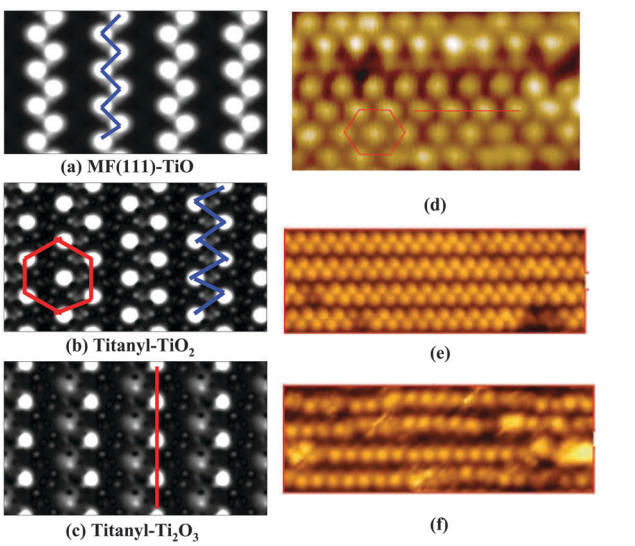

Fig. 4 Simulated STM images of (a) MF(111)-TiO, (b) titanyl-TiO_2 and (c) titanyl-Ti_2O_3, where STM features are highlighted. (d) STM image of the reported R-TiO_2(011)-(2 × 1) structure with a reduced band gap;[14] (e and f) are the STM images of R-TiO_2(011)-(2 × 1) structures before and after irradiation with 300 eV electrons,[13] respectively.

3.4 Thermodynamic stability of R-TiO_2(011) structures

As shown in Fig. 5, the unreconstructed R-TiO_2(011) surface is stable at higher values of the oxygen partial pressure and at lower temperatures. And under these conditions, it competes with the B(001)-TiO_2 reconstruction, in clear agreement with the experimental finding that both surface structures are formed under similar conditions.[10,14,20,47] The formation energies of MF(110)-TiO and MR-TiO reconstructions are nearly equal (Fig. 1), and thus they would be also formed under similar conditions (corresponding to the dark gray region).

The MF(111)-TiO and MR-TiO reconstructions are stable at higher temperatures in ultrahigh vacuum, corresponding to light and dark gray regions, respectively. Theoretically, the unreconstructed R-TiO_2(011) surface would transform into the MF(111)-TiO, or into the MR-TiO reconstructed structures through raising the temperature (as illustrated by line I) or tuning the partial pressure of oxygen gas (as illustrated by line II), respectively.

3.5 Electronic structures of R-TiO_2(011)-(2 × 1) reconstructions

The electronic structures of R-TiO_2(011) reconstructions, determined by their atomic configurations, closely relate to their functionality. To study the effects of reconstructions on photocatalytic reactions, we computed the electronic densities of states (DOS) and band structures.

The DOS of the unreconstructed R-TiO_2(011) surface (Fig. 6a) shows small peaks near the edge of the valence band, in agreement with a previous study.[37] The sharpness of DOS peaks at −1.0 and −1.7 eV is due to the similarity of surface Ti–O bond lengths. For the B(001)-TiO_2 reconstruction (Fig. 6b), these DOS peaks are broadened, indicating the asymmetry of surface bond lengths (1.84 and 1.93 Å).

For the MF(111)-TiO reconstruction (Fig. 6c), new spin-polarized states near the Fermi level appear due to the deficiency of oxygen, corresponding to excess electrons of surface Ti^{3+} ions. The induced magnetic moment is 2.00 μ_B per surface unit cell, while the unreconstructed R-TiO_2(011) surface and B(001)-TiO_2 reconstruction have zero magnetic moment, in agreement with their perfect stoichiometries. In contact with an environment, excess electrons of MF(111)-TiO reconstruction, corresponding to a smaller chemical potential of electrons, would transfer to foreign molecules (*e.g.*, H_2O molecules[37]), and the occupation of antibonding orbitals would facilitate molecular dissociation. According to these results, the relationship between chemical reactivity and surface reconstruction is so close that the multi-functionality of the R-TiO_2(011) face should be attributed to the rich structures of the R-TiO_2(011)-(2 × 1) reconstruction.

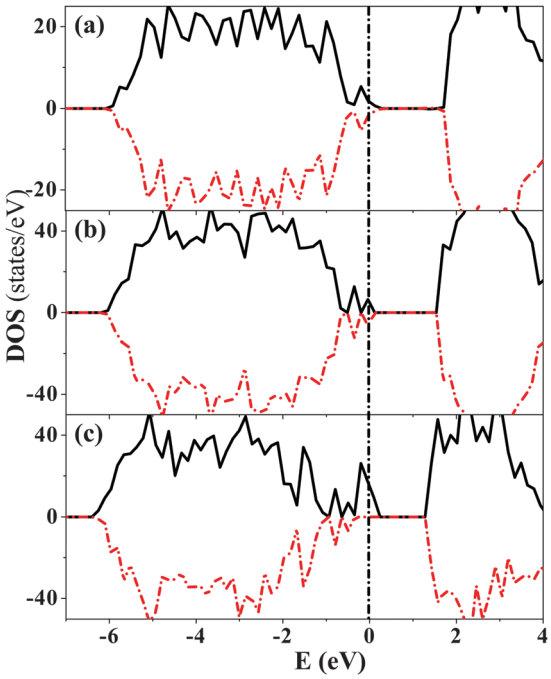

Fig. 6 Densities of states for (a) the unreconstructed R-TiO_2(011) surface, (b) B(001)-TiO_2 and (c) MF(111)-TiO reconstructed structures. The top of the valence band is set to be the zero energy and is denoted by the vertical dashed line.

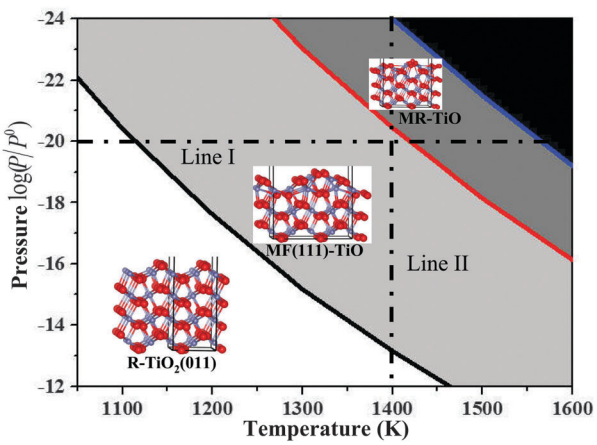

Fig. 5 Phase diagram of R-TiO_2(011) structures. The black region corresponds to the deposition of Ti metal.

The calculated band gap of R-TiO_2 bulk (Fig. 7a) is 2.3 eV, the experimental value being 3.0 eV.[48] Certainly, several approaches that improve the band gaps calculated using the GGA or GGA+*U* methods have been developed, such as hybrid functionals and Green's-function-based methods.[49,50] However, the computational cost of these methods is hundreds of times that of the GGA or GGA+*U* method, and they are not suitable for large systems studied in this paper.

The band gap of titanyl-TiO_2 reconstructed structure (1.7 eV) is 0.6 eV narrower than that of bulk R-TiO_2, in qualitative agreement with Tao's report.[14] This again supports our suggestion that the titanyl-TiO_2 structure is the experimentally discovered R-TiO_2(011)-(2 × 1) reconstruction with reduced band gap.[14] The titanyl-Ti_2O_3 (Fig. 7c) and MF(111)-TiO (Fig. 7d) reconstructions have a computed band gap of 1.30 eV. Considering the under-estimation of calculation, their band gaps should be 2.0 eV. Consequently, these two surface structures, matching with the energy of visible light, could be used for optimizing photoactive responses, approving a previous proposal.[13]

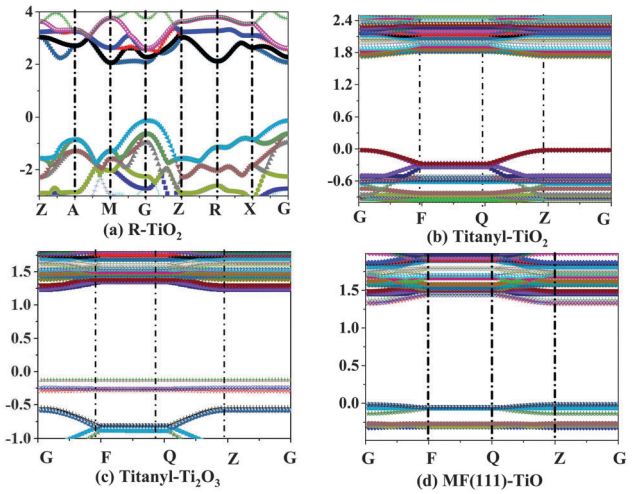

Fig. 7 Band structures of (a) bulk R-TiO_2, (b) titanyl-TiO_2, (c) titanyl-Ti_2O_3 and (d) MF(111)-TiO reconstructions.

4 Conclusions and discussion

In this paper, we found that reconstructions of the (011) surface of TiO_2 rutile are unexpectedly rich, their formation being driven by the combination of thermodynamic conditions and surface stress release. Through detailed analyses, structural uncertainties have been completely solved. First, previous experimental findings[13,14] have been rationalized by the titanyl-TiO_2 and titanyl-Ti_2O_3 reconstructions, due to the agreement of STM images and of the changes in band gaps. Second, the presently predicted MF(111)-TiO reconstruction is more reasonable than the previously proposed MF(111)-TiO_3[11] model from the viewpoint of thermodynamics.

As reported,[51] half of O(Ti) atoms at the surface of the unreconstructed R-TiO_2(110) are twofold (fivefold) coordinated, while all the O(Ti) atoms at the surface are twofold (fivefold) coordinated for the unreconstructed (011) surface. According to the coordination number of surface atoms, the unreconstructed R-TiO_2(011) surface should have a larger surface stress when compared with the unreconstructed (110) surface. Probably the larger surface stress leads to richer structures of the R-TiO_2(011)-(2 × 1) reconstruction. These structures not only correspond to the multifunctionality of the R-TiO_2(011) surface,[3–5] but also help one to clarify the origin of the Brønsted acidity of R-TiO_2. As is well known, the point of zero proton charge is of 4.5–5.5 for R-TiO_2,[52] meaning that the TiO_2 surface binds hydroxyl groups. However, whether H_2O molecules dissociate at the H_2O/TiO_2(110) interface is still under debate.[53–55] The origin of the Brønsted acidity of R-TiO_2 remains a mystery at the atomic level, despite its importance in clarifying the mechanisms of photocatalytic water splitting and degradation of organic pollutants. As was reported, the Brønsted acidity of metal oxides can be understood on the basis of bond-valence theory *via* quantitative structure–activity relationships.[56] Hopefully, the Brønsted acidity of R-TiO_2 can be better understood at the atomic level after the clarification of the R-TiO_2(011) surface structures. Here we take a step forward.

Acknowledgements

This research was supported by the Government of the Russian Federation (grant no. 14.A12.31.0003). Qinggao Wang acknowledges the National Natural Science Foundation of China (Grant No. 11504004) and the "5top100" postdoctoral fellowship conducted at Moscow Institute of Physics and Technology. Calculations were performed on the Rurik supercomputer of our laboratory at Moscow Institute of Physics and Technology.

References

1 A. L. Linsebigler, G. Lu and J. T. Yates, *Chem. Rev.*, 1995, **95**, 735–758.
2 H. Tada, T. Mitsui, T. Kiyonaga, T. Akita and K. Tanaka, *Nat. Mater.*, 2006, **5**, 782–786.
3 J. B. Lowekamp, G. S. Rohrer, P. A. Morris Hotsenpiller, J. D. Bolt and W. E. Farneth, *J. Phys. Chem. B*, 1998, **102**, 7323–7327.
4 P. A. Morris Hotsenpiller, J. D. Bolt, W. E. Farneth, J. B. Lowekamp and G. S. Rohrer, *J. Phys. Chem. B*, 1998, **102**, 3216–3226.
5 T. Ohno, K. Sarukawa and M. Matsumura, *New J. Chem.*, 2002, **26**, 1167–1170.
6 F. Finocchi, A. Barbier, J. Jupille and C. Noguera, *Phys. Rev. Lett.*, 2004, **92**, 136101.
7 G. Jacek, F. Fabio and N. Claudine, *Rep. Prog. Phys.*, 2008, **71**, 016501.
8 N. Claudine, *J. Phys.: Condens. Matter*, 2000, **12**, R367.
9 O. Dulub, C. D. Valentin, A. Selloni and U. Diebold, *Surf. Sci.*, 2006, **600**, 4407–4417.
10 X.-Q. Gong, N. Khorshidi, A. Stierle, V. Vonk, C. Ellinger, H. Dosch, H. Cheng, A. Selloni, Y. He, O. Dulub and U. Diebold, *Surf. Sci.*, 2009, **603**, 138–144.
11 T. Kubo, H. Orita and H. Nozoye, *J. Am. Chem. Soc.*, 2007, **129**, 10474–10478.
12 C. L. Pang, A. Yurtsever, J. Onoda, Y. Sugimoto and G. Thornton, *J. Phys. Chem. C*, 2014, **118**, 23168–23174.
13 O. Dulub, M. Batzilln, S. Solovev, E. Loginova, A. Alchagirov, T. E. Madey and U. Diebold, *Science*, 2007, **317**, 1052–1056.
14 J. Tao, T. Luttrell and M. Batzill, *Nat. Chem.*, 2011, **3**, 296–300.
15 T. J. Beck, A. Klust, M. Batzill, U. Diebold, C. Di Valentin and A. Selloni, *Phys. Rev. Lett.*, 2004, **93**, 036104.
16 T. J. Beck, A. Klust, M. Batzill, U. Diebold, C. Di Valentin, A. Tilocca and A. Selloni, *Surf. Sci.*, 2005, **591**, L267–L272.
17 C. Di Valentin, A. Tilocca, A. Selloni, T. J. Beck, A. Klust, M. Batzill, Y. Losovyj and U. Diebold, *J. Am. Chem. Soc.*, 2005, **127**, 9895–9903.
18 X. Torrelles, G. Cabailh, R. Lindsay, O. Bikondoa, J. Roy, J. Zegenhagen, G. Teobaldi, W. A. Hofer and G. Thornton, *Phys. Rev. Lett.*, 2008, **101**, 185501.
19 S. E. Chamberlin, C. J. Hirschmugl, H. C. Poon and D. K. Saldin, *Surf. Sci.*, 2009, **603**, 3367–3373.
20 T. Woolcot, G. Teobaldi, C. L. Pang, N. S. Beglitis, A. J. Fisher, W. A. Hofer and G. Thornton, *Phys. Rev. Lett.*, 2012, **109**, 156105.

21 U. Diebold, *Nat. Chem.*, 2011, **3**, 271–272.
22 C. B. Duke, *Chem. Rev.*, 1996, **96**, 1237–1259.
23 R. J. Needs, M. J. Godfrey and M. Mansfield, *Surf. Sci.*, 1991, **242**, 215–221.
24 W. Haiss, *Rep. Prog. Phys.*, 2001, **64**, 591.
25 Q. Wang, A. R. Oganov, Q. Zhu and X.-F. Zhou, *Phys. Rev. Lett.*, 2014, **113**, 266101.
26 M. Lazzeri and A. Selloni, *Phys. Rev. Lett.*, 2001, **87**, 266105.
27 A. R. Oganov and C. W. Glass, *J. Chem. Phys.*, 2006, **124**, 244704.
28 A. R. Oganov, A. O. Lyakhov and M. Valle, *Acc. Chem. Res.*, 2011, **44**, 227–237.
29 Q. Zhu, L. Li, A. R. Oganov and P. B. Allen, *Phys. Rev. B: Condens. Matter Mater. Phys.*, 2013, **87**, 195317.
30 A. O. Lyakhov, A. R. Oganov, H. T. Stokes and Q. Zhu, *Comput. Phys. Commun.*, 2013, **184**, 1172–1182.
31 V. Sharma, C. Wang, R. G. Lorenzini, R. Ma, Q. Zhu, D. W. Sinkovits, G. Pilania, A. R. Oganov, S. Kumar, G. A. Sotzing, S. A. Boggs and R. Ramprasad, *Nat. Commun.*, 2014, **5**, 4845.
32 G. Kresse and J. Hafner, *Phys. Rev. B: Condens. Matter Mater. Phys.*, 1993, **48**, 13115–13118.
33 G. Kresse and J. Furthmuller, *Phys. Rev. B: Condens. Matter Mater. Phys.*, 1996, **54**, 11169–11186.
34 G. Kresse and J. Furthmuller, *Comput. Mater. Sci.*, 1996, **6**, 15–50.
35 A. J. Cohen, P. Mori-Sanchez and W. Yang, *Science*, 2008, **321**, 792–794.
36 N. A. Deskins, R. Rousseau and M. Dupuis, *J. Phys. Chem. C*, 2009, **114**, 5891–5897.
37 U. Aschauer and A. Selloni, *Phys. Rev. Lett.*, 2011, **106**, 166102.
38 P. E. Blochl, *Phys. Rev. B: Condens. Matter Mater. Phys.*, 1994, **50**, 17953–17979.
39 J. Neugebauer and M. Scheffler, *Phys. Rev. B: Condens. Matter Mater. Phys.*, 1992, **46**, 16067–16080.
40 G. Makov and M. C. Payne, *Phys. Rev. B: Condens. Matter Mater. Phys.*, 1995, **51**, 4014–4022.
41 W. Qing-Gao and S. Jia-Xiang, *J. Phys.: Condens. Matter*, 2012, **24**, 225005.
42 NIST, Chemistry Webbook. http://webbook.nist.gov/.
43 D.-J. Shu, S.-T. Ge, M. Wang and N.-B. Ming, *Phys. Rev. Lett.*, 2008, **101**, 116102.
44 R. J. Needs, *Phys. Rev. Lett.*, 1987, **58**, 53–56.
45 Q.-G. Wang, J.-X. Shang and Z. Yang, *J. Phys. Chem. C*, 2012, **116**, 23371–23376.
46 J. Tersoff and D. R. Hamann, *Phys. Rev. B: Condens. Matter Mater. Phys.*, 1985, **31**, 805–813.
47 J. M. R. Muir and H. Idriss, *Surf. Sci.*, 2013, **607**, 187–196.
48 U. Diebold, *Surf. Sci. Rep.*, 2003, **48**, 53–229.
49 J. Heyd, J. E. Peralta, G. E. Scuseria and R. L. Martin, *J. Chem. Phys.*, 2005, **123**, 174101.
50 J. E. Peralta, J. Heyd, G. E. Scuseria and R. L. Martin, *Phys. Rev. B: Condens. Matter Mater. Phys.*, 2006, **74**, 073101.
51 H. Perron, C. Domain, J. Roques, R. Drot, E. Simoni and H. Catalette, *Theor. Chem. Acc.*, 2007, **117**, 565–574.
52 J. Cheng and M. Sprik, *J. Chem. Theory Comput.*, 2010, **6**, 880–889.
53 L.-M. Liu, C. Zhang, G. Thornton and A. Michaelides, *Phys. Rev. B: Condens. Matter Mater. Phys.*, 2010, **82**, 161415.
54 L.-M. Liu, C. Zhang, G. Thornton and A. Michaelides, *Phys. Rev. B: Condens. Matter Mater. Phys.*, 2012, **85**, 167402.
55 D. J. Wesolowski, J. O. Sofo, A. V. Bandura, Z. Zhang, E. Mamontov, M. Predota, N. Kumar, J. D. Kubicki, P. R. C. Kent, L. Vlcek, M. L. Machesky, P. A. Fenter, P. T. Cummings, L. M. Anovitz, A. A. Skelton and J. Rosenqvist, *Phys. Rev. B: Condens. Matter Mater. Phys.*, 2012, **85**, 167401.
56 I. D. Brown, K. R. Poeppelmeier and B. Bickmore, *Bond Valences*, Springer, Berlin, Heidelberg, 2014, vol. 158, pp. 191–203.